The PLETHORA Gene Regulatory Network Guides Growth and Cell Differentiation in Arabidopsis Roots[OPEN]

Luca Santuari,[a,b,1] Gabino F. Sanchez-Perez,[b,c,d,1] Marijn Luijten,[e] Bas Rutjens,[a,e] Inez Terpstra,[e,2] Lidija Berke,[d,f] Maartje Gorte,[e] Kalika Prasad,[e,3] Dongping Bao,[e,4] Johanna L.P.M. Timmermans-Hereijgers,[e] Kenichiro Maeo,[g] Kenzo Nakamura,[g] Akie Shimotohno,[e,5] Ales Pencik,[h] Ondrej Novak,[h,6] Karin Ljung,[h] Sebastiaan van Heesch,[i,7] Ewart de Bruijn,[i,j] Edwin Cuppen,[i,k] Viola Willemsen,[a,e] Ari Pekka Mähönen,[e,l] Wolfgang Lukowitz,[m] Berend Snel,[d] Dick de Ridder,[b] Ben Scheres,[a,e,8] and Renze Heidstra[a,e,8]

[a] Plant Developmental Biology, Wageningen University and Research Centre, Wageningen 6708PB, The Netherlands
[b] Bioinformatics Group, Wageningen University and Research Centre, Wageningen 6708PB, The Netherlands
[c] Applied Bioinformatics, Bioscience, Plant Research International, Wageningen University and Research Centre, Wageningen 6708PB, The Netherlands
[d] Theoretical Biology and Bioinformatics, Utrecht University, Utrecht 3584 CH, The Netherlands
[e] Molecular Genetics, Department of Biology, Utrecht University, Utrecht 3584 CH, The Netherlands
[f] Biosystematics Group, Wageningen University and Research Centre, 6708PB Wageningen, The Netherlands
[g] Laboratory of Biochemistry, Graduate School of Bioagricultural Science, Nagoya University, Nagoya 464-8601, Japan
[h] Umeå Plant Science Centre, Department of Forest Genetics and Plant Physiology, Swedish University of Agricultural Sciences, Umeå SE-901 83, Sweden
[i] Hubrecht Institute-KNAW and University Medical Center Utrecht, Utrecht 3584 CT, The Netherlands
[j] Hartwig Medical Foundation, 1098 XH Amsterdam, The Netherlands
[k] Department of Medical Genetics, University Medical Center Utrecht, Utrecht 3584 CX, The Netherlands
[l] Institute of Biotechnology, University of Helsinki, Helsinki 00014, Finland
[m] Department of Plant Biology, University of Georgia, Athens, Georgia 30602-7271

ORCID IDs: 0000-0001-8784-2507 (L.S.); 0000-0003-4476-0987 (M.L.); 0000-0002-3085-2533 (I.T.); 0000-0003-3842-9462 (L.B.); 0000-0003-3452-0154 (O.N.); 0000-0003-2901-189X (K.L.); 0000-0001-6051-866X (A.P.M.); 0000-0002-5864-7240 (W.L.); 0000-0002-5804-8547 (B. Snel); 0000-0002-4944-4310 (D.d.R.); 0000-0001-5400-9578 (B. Scheres); 0000-0001-9032-5770 (R.H.)

Organ formation in animals and plants relies on precise control of cell state transitions to turn stem cell daughters into fully differentiated cells. In plants, cells cannot rearrange due to shared cell walls. Thus, differentiation progression and the accompanying cell expansion must be tightly coordinated across tissues. PLETHORA (PLT) transcription factor gradients are unique in their ability to guide the progression of cell differentiation at different positions in the growing *Arabidopsis thaliana* root, which contrasts with well-described transcription factor gradients in animals specifying distinct cell fates within an essentially static context. To understand the output of the PLT gradient, we studied the gene set transcriptionally controlled by PLTs. Our work reveals how the PLT gradient can regulate cell state by region-specific induction of cell proliferation genes and repression of differentiation. Moreover, PLT targets include major patterning genes and autoregulatory feedback components, enforcing their role as master regulators of organ development.

INTRODUCTION

Plant and animal organ growth require coordination of cell division, growth, and differentiation to maintain tissue integrity. Cells in animal tissues can rearrange by preferential cell-cell interactions, which provide an extra mechanism for tissue-level coordination, but plant cells have fixed positions in the tissue due to shared cell walls, which highlights the importance of positional information to guide cell differentiation. Plant growth is maintained from organized groups of dividing cells in meristems. At the heart of the root meristem lies the stem cell niche where, mitotically less active quiescent center (QC) cells act as an organizer to maintain the surrounding stem cells that in turn produce transit amplifying daughter cells. During growth, cells undergo transitions from division toward expansion and differentiation in distinct developmental zones and interactions between plant growth factors of the auxin and cytokinin classes play an important role in this process (Heidstra and Sabatini, 2014). In addition, root meristem growth factor (RGF) peptides and their receptors (RGFRs) as well as nuclear GROWTH-REGULATING FACTOR (GRF) corepressor proteins regulate meristematic activity by influencing the activity of PLETHORA (PLT) proteins (Matsuzaki et al., 2010; Rodriguez et al., 2015; Ou et al., 2016; Shinohara et al., 2016).

PLT proteins form gradients by mitotic distribution and short distance cell-to-cell movement of the proteins from a stem cell centered transcriptional domain (Mähönen et al., 2014). Expression of *PLT* genes, also called *AINTEGUMENTA-LIKE* (*AIL*) genes, is restricted to developing tissues in roots and shoots, and controls outgrowth and patterning of organ primordia (Prasad et al., 2011; Krizek and Eaddy, 2012; Hofhuis et al., 2013). The PLT/AIL family comprises a subclade of six transcription factors that are members of the double APETALA2/ETHYLENE RESPONSE FACTOR domain family (Aida et al., 2004; Nole-Wilson et al., 2005;

Galinha et al., 2007; Horstman et al., 2014; Mähönen et al., 2014). In the root meristem, four *PLT* members, *PLT1/AIL3*, *PLT2/AIL4*, *PLT3/AIL6*, and *BBM/PLT4/AIL2*, partly overlap in their transcriptional domains and function redundantly to maintain cell division and prevent cell differentiation (Galinha et al., 2007). In addition, these genes are required for the expression of QC markers at the correct position within the stem cell niche (Aida et al., 2004), which also requires the activity of the SHORTROOT-SCARECROW pathway that has a major role in radial tissue patterning (Helariutta et al., 2000; Wysocka-Diller et al., 2000; Nakajima et al., 2001; Sabatini et al., 2003). *PLT3*, *PLT5/AIL5*, and *PLT7/AIL7* are expressed in lateral root founder cells and in the shoot apical meristem, where they function redundantly in the positioning and outgrowth of lateral organs (Prasad et al., 2011; Hofhuis et al., 2013). In addition, PLT2, BBM/PLT4, and PLT5 have the remarkable capacity to ectopically initiate the formation of specific organs and somatic embryos (Boutilier et al., 2002; Galinha et al., 2007; Tsuwamoto et al., 2010). In line with the observed genetic redundancy in the PLT/AIL clade, similar DNA binding sites for PLT1 and PLT3 have been reported based on DNA affinity purification sequencing (DAP-seq) (O'Malley et al., 2016), and PLT5 was shown to be able to bind an ANT binding consensus sequence by electrophoretic mobility shift assay (Nole-Wilson and Krizek, 2000; Yano et al., 2009).

The PLT proteins involved in regulating division and differentiation are expressed in a gradient within the primary root, act in a dose-dependent manner (Galinha et al., 2007), and their local concentration defines thresholds for cell division and differentiation (Mähönen et al., 2014). Here, we investigate large-scale transcriptional programs redundantly regulated by the PLT proteins and show that they promote transcription of cell division and growth-related genes in their expression domain and repress differentiation genes. We determine direct targets and show that PLTs act as direct activators of cell division and growth programs through similar binding motifs. Collectively, our data indicate how transcriptional activation and repression can translate the PLT

[1] These authors contributed equally to this work.

[2] Current address: RNA Biology and Applied Bioinformatics, Swammerdam Institute for Life Sciences, University of Amsterdam, Amsterdam 1098 XH, The Netherlands.

[3] Current address: School of Biology, Indian Institute of Science Education and Research, Thiruvananthapuram 695016, India.

[4] Current address: National Institute of Education, Nanyang Technological University, Singapore 637616.

[5] Current address: Department of Biological Sciences, Graduate School of Science, University of Tokyo, 7-3-1 Hongo, Bunkyo-ku, Tokyo 113-0033, Japan.

[6] Current address: Laboratory of Growth Regulators and Department of Chemical Biology and Genetics, Palacký University and Institute of Experimental Botany ASCR, Olomouc 783 71, Czech Republic.

[7] Current address: Experimental Genetics of Cardiovascular Diseases, Max-Delbrück-Center for Molecular Medicine, Berlin 13125, Germany.

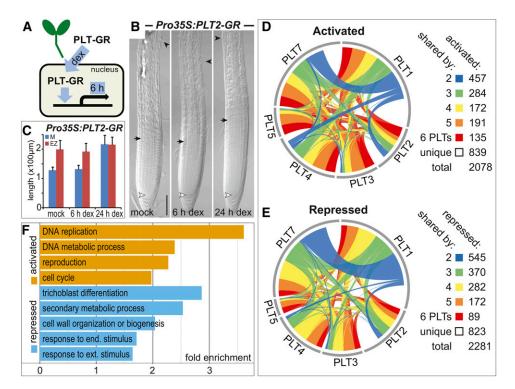[8] Address correspondence to ben.scheres@wur.nl or renze.heidstra@wur.nl.

The author responsible for distribution of materials integral to the findings presented in this article in accordance with the policy described in the Instructions for Authors (www.plantcell.org) is: Renze Heidstra (renze.heidstra@wur.nl).

gradient in different output domains, suggesting how this gradient can coordinate growth, division, and differentiation.

RESULTS

PLTs Regulate a Common Set of Genes

The overlapping expression domains of PLT transcription factors together with protein sequence similarity in DNA binding domains and partial genetic redundancy suggest that they share targets. In support of a common set of targets, we confirmed and extended previous experiments by showing that each *PLT* member, when driven by the *PLT2* promoter, can (partially) rescue the short root phenotype of the *plt1 plt2* double mutant (Galinha et al., 2007) (Supplemental Figure 1A).

To identify genes regulated by each PLT member independent of their expression domain, we employed a constitutive promoter-driven inducible system in which PLT is fused to the glucocorticoid receptor (GR; Schena et al., 1991) hormone binding domain (Pro35S:PLT-GR). The PLT-GR fusions are sequestered in the cytoplasm and 6 h after dexamethasone (DEX)-induced nuclear translocation, we profiled gene expression changes in whole seedlings (Figure 1). In this time frame, roots do not show the typical zonation changes that are observed after prolonged induction of each of the PLT genes (Figures 1B and 1C; Supplemental Figures 1B and 1C). Interestingly, each gene set regulated by a distinct PLT protein consisted of about equal amounts of activated and repressed genes, suggesting that PLT transcription factors have two distinct roles (Supplemental Figure 1D and Supplemental Data Set 1). The data further indicated that PLTs regulate a common set of genes, with 62% shared by at least two PLTs and 39% shared by at least three (Figures 1D and 1E; Supplemental Figure 1E and Supplemental Data Set 1). Gene Ontology (GO) term enrichment analysis on the pooled activated genes supported the role of PLTs in promoting primary growth processes, such as DNA replication, DNA metabolism, and cell cycle regulation (Figure 1F; Supplemental Data Set 2). Repressed genes, instead, were enriched for categories related to cell expansion and differentiation, such as cell wall biogenesis or organization, and trichoblast differentiation (Figure 1F; Supplemental Data Set 2). Interestingly, we noted some of the same defense-related categories for PLT-repressed genes as the recent transcriptomics profiling study on the *ant plt3* double mutant inflorescences, suggesting a role for PLT/AIL genes in controlling defense pathways (Krizek et al., 2016).

The PLT Gradient Separates Transcriptional Responses in the Root

PLT1, PLT2, PLT3, and BBM/PLT4 concentrations in the primary root are at the highest level in the stem cell niche and progressively decrease along the cell division zone until cells reach the expansion and differentiation zone. PLT activity controls each of these zone boundaries (Aida et al., 2004; Galinha et al., 2007; Mähönen et al., 2014). Given the shape and function of the PLT gradient and the similar numbers of downstream activated and repressed genes, we asked whether PLT-regulated genes were expressed at different specific locations in the root. We mapped all PLT-regulated genes on an established gene expression atlas of the root (Brady et al., 2007) that provides both a longitudinal and a tissue-level perspective.

Figure 1. PLTs Activate and Repress Shared Gene Sets.

(A) Schematic representation of the induction experiment to identify genes regulated by each PLT protein. Constitutively expressed PLT-GR fusions sequestered in the cytoplasm were translocated to the nucleus upon DEX induction followed by gene expression profiling after 6 h in whole seedlings.
(B) Roots display meristem expansion only after 6 h of DEX-induced Pro35S:PLT2-GR overexpression. The meristem zone from QC (white arrowhead) to the first rapidly elongating cortex cell (black arrow) is followed by the elongation zone up to the first emerging root hair (black arrowhead). Five-day-old seedlings. Bar = 50 μm.
(C) Quantification of meristem (M) and elongation zone (EZ) size in roots in time upon DEX-induced Pro35S:PLT2-GR overexpression. Means + SD are represented.
(D) and **(E)** Overlap among gene sets activated **(D)** and repressed **(E)** by each PLT-GR fusion protein upon 6 h of DEX induction (Supplemental Data Set 1). Link width signifies the number of shared regulated genes.
(F) Selected significant GO terms for PLT-regulated genes (Supplemental Data Set 2). P < 2.04 × 10^{-16}, Fisher's exact test.

PLT-activated genes are preferentially expressed in the meristem division zone (1303 out of 2028 genes [64%] show highest expression in L1-6), while PLT-repressed genes mostly show highest expression outside of the PLT gradient domain, in the elongation and differentiation zones (1317 out of 2221 genes [59%] show highest expression in L7-12) (Figure 2). These results are consistent with the GO analysis indicating PLT-mediated growth promoting effects. Activated genes with highest expression in the differentiation zone (L7-L12) are mostly related to auxin biosynthesis and metabolism (Supplemental Data Set 2), suggestive of their activation by PLT during the lateral root initiation processes. Focusing on the repressed genes with the highest expression in the meristem (L1-L6) delivered GO terms related to differentiation consistent with gradual derepression of differentiation-related genes (Supplemental Data Set 2).

The columella (Col) section represents root cap tissue consisting of both dividing and differentiating cells (Brady et al., 2007), explaining the presence of both PLT-activated (315 out of 2028 genes [16%] show highest expression in Col) and PLT-repressed genes (395 out of 2221 genes [18%] show highest expression in Col).

Interestingly, we noted a pronounced accumulation of PLT-activated genes in the L2, whereas *PLT* transcript and PLT protein levels peak around the QC region within the L1 (Figure 2A; Mähönen et al., 2014). Plotting these PLT-activated genes at the tissue-specific level shows accumulation of genes expressed in the meristematic xylem (S4) not correlated with *PLT* transcript accumulation (Supplemental Figure 2), suggesting either the involvement of cooperative tissue-specific factors that regulate these gene expression patterns or that these represent secondary response genes. These results support the role of PLTs in promoting cell division and inhibiting cell differentiation along the root, translating gradient information into transcriptional changes that guide zonation.

PLTs Regulate Auxin Biosynthesis and Transport in the QC

The expression of PLT1, PLT2, PLT3, and BBM/PLT4 peaks in the QC that acts as a stem cell organizer at the center of the root stem cell niche. To probe the physiological response in these highly specialized cells, we chose to test PLT2 because of the dramatic
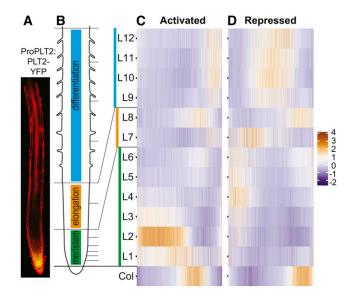
Figure 2. PLT Guides Large-Scale Region-Specific Transcriptional Activation and Repression.

(A) Root showing gradient expression of ProPLT2:PLT2-YFP.

(B) Schematic of a root depicting developmental zones in color. Horizontal lines correspond to sections (L1-L12) of the longitudinal Root Gene Expression Atlas (Brady et al., 2007). The root in **(A)** is aligned to largely match zones and sections in **(B)**.

(C) and **(D)** Expression profile (z-score) of genes (x axis) activated **(C)** or repressed **(D)** by at least one PLT in longitudinal sections according to the Root Gene Expression Atlas (Brady et al., 2007) (Supplemental Data Set 1). Col tissue consists of both dividing and differentiating cells.

phenotypes conferred upon its ectopic expression and in knockout combinations with other *PLT* members (Galinha et al., 2007). We employed the inducible PLT2-GR fusion, under its native promoter, to identify PLT2-regulated genes in the QC in the *plt1 plt2* background (Figure 3). Following 1 and 4 h of DEX induction, QC cells were isolated by cell sorting using the *WUSCHEL-RELATED HOMEOBOX5* (*WOX5*; Sarkar et al., 2007) promoter-driven GFP that stably marks the *plt1 plt2* mutant QC region (Supplemental Figure 3A). The expression analysis revealed a significant overlap between regulated genes obtained from this physiological QC experiment and those from the whole seedlings using overexpression (activated genes, $P < 1.1 \times 10^{-85}$; repressed genes, $P < 3 \times 10^{-38}$, Fisher's exact test) (Figure 3B; Supplemental Data Set 1). Notably, this indicates that PLT-mediated activation and repression of targets first identified by induced overexpression operate under physiological conditions. PLT2-induced genes in the QC region included the polar auxin transport gene *PIN4*, consistent with previous data (Blilou et al., 2005; Galinha et al., 2007). GO analysis on QC-activated genes revealed a significant enrichment for categories related to auxin and glucosinolate biosynthesis and metabolism genes, such as *YUCCA3* (*YUC3*) (Supplemental Figure 3B and Supplemental Data Sets 1 and 2), supporting the proposed role for PLT in regulating auxin biosynthesis and accumulation (Pinon et al., 2013). To test whether PLT activity can modulate auxin biosynthesis and accumulation in roots, we measured indole acetic acid (IAA) levels in *plt1 plt2* versus wild-type root tips and observed a lower IAA level in

the root tips of 6-d-old *plt1 plt2* seedlings compared with wild-type seedlings (Figure 3C). Consistently, the Pro35S:PLT2-GR lines displayed enhanced IAA biosynthesis rates and concentrations in the root tips after DEX induction (Figure 3D; Supplemental Figure 3C). These results indicate that auxin-induced PLTs in turn regulate auxin accumulation in the QC both through transport and biosynthesis.

PLT and Auxin Transcriptional Response Partially Overlap

The PLT protein gradient in the root tip depends on high and prolonged auxin accumulation, and auxin can only slowly regulate gradient shape, desensitizing the gradient to immediate auxin responses (Mähönen et al., 2014). However, whether auxin might exert part of its fast effects on growth by modulating PLT activity at the protein level remained hitherto unknown. In the latter case, all PLT-regulated genes should be a subset of auxin-responsive genes. A comparison between PLT-regulated genes and two data sets of auxin-responsive genes in the root (Bargmann et al., 2013; Lewis et al., 2013) revealed that, although a significant proportion of genes displays a coherent joint regulation by PLTs and auxin, 70% of PLT activated genes and 64% of PLT repressed genes were unaffected by auxin treatment (Figures 3E and 3F; Supplemental Figures 4A and 4B and Supplemental Data Set 3). This excludes the possibility that auxin generally modifies PLT protein activity. The overlapping genes were in large part induced within 2 h of auxin treatment in the time-resolved auxin response data set (Lewis et al., 2013) (Supplemental Figures 4C and 4D). Interestingly, the overlapping genes clustered to the meristem-expressed L2/S4 profile on the gene expression atlas of the root (Brady et al., 2007) (Supplemental Figure 4E), with over-represented GO terms for growth processes (Lewis et al., 2013). Given the conspicuous enrichment of auxin biosynthesis genes in the QC after complementation reported above, this overlap may in part be caused by PLT-induced auxin production in roots.

PLT2 Binds Major Regulators of Embryonic Patterning and Root Development

To understand how the PLTs control gene regulation, we performed genome-wide analysis of PLT2-bound genes in root tissue, defining these as PLT2 targets. Chromatin immunoprecipitation was followed by sequencing (ChIP-seq) (Johnson et al., 2007) on *ProPLT2:PLT2-YFP* complemented *plt1 plt2* root tissues (Figure 3A). We identified 2482 genomic regions enriched for PLT2 binding (peaks; Supplemental Data Set 4). Considering the overlap in genes regulated by PLTs, we asked whether this was reflected in common binding positions. A comparison with a ChIP-seq data set from *ProBBM:BBM-YFP*-expressing somatic embryos (Horstman et al., 2015) revealed a highly significant overlap (51% of PLT2 binding peaks: P = 0.001 [poverlap]; Supplemental Data Set 4), indicating that genome binding regions of distinct PLT proteins overlap.

The PLT2 peak summits were assigned to the closest gene within 4 kb of its transcription start site (TSS). Thus, assigned target genes represented 30% of the PLT2-activated genes (Figure 4 A, pink, 200 genes; Supplemental Data Set 5) and 10% of the PLT2-repressed genes (Figure 4B, blue, 96 genes;
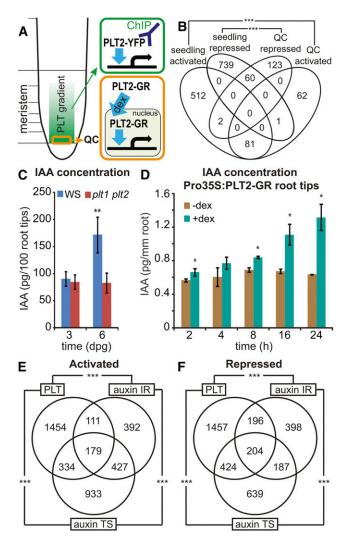
Figure 3. PLT2 Regulates Auxin Biosynthesis and Response Genes.

(A) Schematic overview of PLT2-YFP ChIP-seq (green) and PLT2-GR regulated QC transcriptomics (orange) experiments.

(B) Venn diagram showing the overlap among regulated genes obtained from seedlings upon induced Pro35S:PLT2-GR overexpression and regulated genes from QC upon physiological complementation of *plt1 plt2* by induction of ProPLT2:PLT2-GR (Supplemental Data Set 1). Regulated genes from 1 and 4 h DEX time points were pooled for the QC data set. Activated genes, ***P < 1.1 × 10^{-85}; repressed genes, ***P < 3 × 10^{-38}; Fisher's exact test.

(C) IAA levels in root tips (2 mm) at 3 and 6 d after germination in wild-type (Ws) and *plt1 plt2* double mutant plants. Samples were measured in quintuples. **P < 0.0008, Student's *t* test. Error bars indicate SD.

(D) IAA levels in 6-d-old Pro35S:PLT2-GR root tips (2 mm) after 2, 4, 8, 16, and 24 h mock treatment compared with DEX induction. Measurements were performed in triplicate per time point with 50 root tips per sample. *P < 0.05, Student's *t* test. Error bars indicate SD.

(E) and **(F)** Overlap between genes activated **(E)** and repressed **(F)** by PLTs and the auxin intact root (IR; Bargmann et al., 2013) and time series (TS; Lewis et al., 2013) gene sets (Supplemental Data Set 3). ***P < 2.2 × 10^{-55}, Fisher's exact test.

Supplemental Data Set 5), in line with the results of other transcription factor studies (Lau et al., 2014). In the physiological PLT2 QC data set alone, the proportion of QC-activated targets was 41% (60 genes), while the proportion of QC-repressed targets was 14% (26 genes). A 19% overlap was observed for activated targets both in the QC region and whole seedlings (38 genes), while the overlap for repressed targets was limited to 5% (five genes) (Figures 4A and 4B). Compared with the full set of genes regulated upon PLT overexpression (Figures 2C and 2D), the expression patterns of the PLT2-regulated targets on the gene expression atlas of the root (Brady et al., 2007) revealed an activation profile more in agreement with the expression pattern of PLT2 itself (Figure 4D), whereas the repression profile remained similar (Figure 4E). Specifically, the cluster of L2/S4-regulated genes (Supplemental Figure 2) is largely absent from the activated target gene expression profile (Figure 4D), indicating these represent secondary response genes. Among PLT2-activated targets, several genes have profound roles in embryonic development and postembryonic root zonation (Supplemental Table 1). Some notable examples are the auxin response factor *MONOPTEROS* (*ARF5/MP*) (Hardtke and Berleth, 1998), the CDK inhibitor *ICK3/KRP5* (Wen et al., 2013), and the GATA transcription factor *HANABA TARANU* (*HAN*) (Nawy et al., 2010) (Figure 4C). In addition, auxin biosynthesis genes *YUC3* and *YUC8* represent PLT2-activated targets (Supplemental Data Sets 1 and 4) that, together with the observed regulation of *YUC4* in the shoot by PLT5-GR in the presence of the protein synthesis inhibitor cyclohexamide (Pinon et al., 2013), shows that the PLT proteins are direct regulators of auxin biosynthesis.

Direct Activation and Repression through Distinct Mechanisms

Tests in yeast with PLT1 and BBM/PLT4 indicate that PLTs represent transcriptional activators (Horstman et al., 2015) (Supplemental Figure 5). PLT2 preferentially binds upstream and close to the TSS (Figure 4F; 70 and 22% within 3 and 500 bp, respectively; Supplemental Data Set 4). Activated targets preferentially bound PLT2 within 500 bp upstream of their TSS (false discovery rate [FDR] < 5%) (Figure 4G). Our results suggest that PLT2 activates its targets by binding to the core promoter region, resulting in their meristematic expression. PLT2 binding of repressed targets is more diffuse with respect to the TSS and barely enriched when compared with the simulated random distribution (Figure 4H). Overall, we concluded that nearly one-fifth (19%) of PLT2 targets is regulated in the seedling context and that PLT2 activates transcription through readily distinguishable binding events. Repression is either indirect or occurs through less well defined positions. qRT-PCR analysis confirmed that targets respond to PLT2 induction (Figure 4I). In addition, we generated several promoter-erGFP (endoplasmic reticulum-targeted GFP) fusions (Supplemental Figure 5) of PLT2-regulated target genes to test whether genes are activated in different domains of the PLT2 gradient. From these we chose *ProYUC3*, *ProTLP8* (*Tubby-like protein 8*), and *ProRCH1* promoter fusion expressed in consecutive regions in the root meristem and analyzed their activation in a DEX-induced ProPLT2:PLT2-GR complementation assay in the
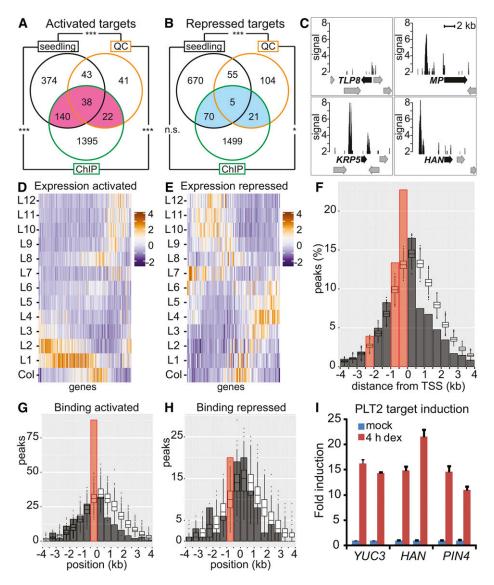
Figure 4. Genome-Wide Analysis of PLT2 Binding to Target Genes.

(A) and **(B)** PLT2-activated targets (**[A]**; pink) and repressed targets (**[B]**; blue). Overlap between genes bound (ChIP) and transcriptionally regulated by PLT2 (seedlings and QC) represent regulated targets (Supplemental Data Set 5). ***$P < 7.6 \times 10^{-29}$ and *$P < 0.005$; Fisher's exact test. n.s., not significant.

(C) PLT2 ChIP-seq profiles of selected regulated targets. Peak signal (CSAR score) plotted with a minimum of 2. Arrows represent genes; black arrows indicate annotated gene for PLT2 ChIP-seq peak.

(D) and **(E)** Expression profile (z-score) according to the Root Gene Expression Atlas (Brady et al., 2007) of PLT2-activated **(D)** and -repressed **(E)** targets from **(A)** (pink) and **(B)** (blue), respectively.

(F) Proportion of PLT2 peaks (bars, summit positions were considered) located relative to the closest TSS over the number of peaks assigned within 4 kb (2381 out of a total of 2482 peaks). Box plots show distributions obtained by random selections of genomic positions and assignment to the closest TSS. The x axis displays position of 500-bp genomic bins relative to the TSS within 4 kb. Red bar: significantly enriched over simulated random distribution, FDR < 5%. The shape of the simulated distribution reflects the high gene density of the Arabidopsis genome.

(G) and **(H)** Number of PLT2 peaks (bars) compared with the simulated distribution of random positions (box plots) relative to the distance from the TSS (0) for PLT2-activated **(G)** and -repressed **(H)** targets from **(A)** (pink) and **(B)** (blue), respectively. Width of bars and box plots represent 500-bp genomic bins around the TSS. Red bar indicates significantly enriched over simulated random distribution, FDR < 5%.

(I) qRT-PCR analysis of PLT2 target induction. Expression levels of *YUC3*, *HAN*, and *PIN4* transcripts in root tips after 4 h DEX induction of Pro35S: PLT2-GR compared with the mock-treated condition. Data represent biological duplicates with each time point consisting of technical triplicates. Error bars indicate SE.
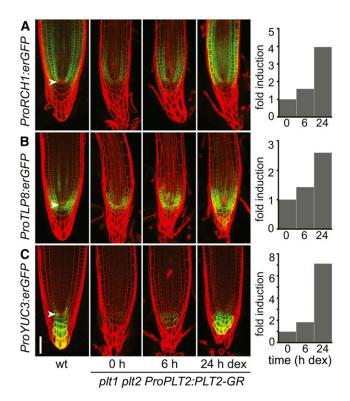
Figure 5. PLT2 Activates Promoters in Distinct Parts of the Root.

Activation of ProRCH1:erGFP **(A)**, ProTLP8:erGFP **(B)**, and ProYUC3:erGFP **(C)** expression in root tips after 0, 6, and 24 h of DEX induction of ProPLT2:PLT2-GR in 5-d-old *plt1 plt2* seedlings. The 0 h time point reflects the lower expression in the *plt1 plt2* mutant. The erGFP expression pattern is compared with that in a wild-type background. Expression of erGFP was quantified in representative depicted transformants and plotted in fold change of erGFP levels relative to the uninduced (0 h) situation. For each induction series, a transgenic root is followed in time and depicted using identical confocal settings and the same medial focal plane. Experiments were repeated four times (ProRCH1:erGFP), 12 times (ProTLP8:erGFP), and nine times (ProYUC3:erGFP). Arrowhead indicates QC. Bar = 50 μm.

plt1 plt2 mutant background. The results show that PLT2 activates each of these promoters in their own domain of expression (Figure 5), suggesting that the PLT gradient cooperates with tissue-specific factors to regulate individual gene expression patterns.

To investigate the importance of the gradient expression of PLT2 for target gene regulation, we followed over time the activation of the promoter of *TLP8* (Lai et al., 2004), *YUC3* (Zhao et al., 2001), and *HAN* (Nawy et al., 2010) genes driving a fluorescent reporter gene upon DEX induction of PLT2-GR expressed under control of the constitutive 35S promoter (Figure 6; Supplemental Figure 6). Ectopic induction of these promoters is obvious within 6 h of transfer to DEX media from the enhanced expression of fluorescent protein throughout the root outside of the meristematic domain of endogenous PLT2 expression. A further increase in expression at 24 h after DEX activation of PLT2-GR is accompanied with the typical enlarged meristem size phenotype but extends well beyond this shifted zone boundary (Figure 6; Supplemental Figure 6). Therefore, at least in a subset of regulated targets, PLT levels determine the proximal/shootward boundary

of the target gene expression domain, consistent with a dose-dependent role in zonation.

PLTs Recognize an ANT-Like Motif

De novo motif discovery with MEME (Bailey and Elkan, 1995) on PLT2 peaks as determined by ChIP-seq returned a motif similar to the DNA binding motifs derived from DAP-seq for PLT1, PLT3, and PLT7 (O'Malley et al., 2016) and the one previously characterized for the close homolog AINTEGUMENTA (ANT) (Nole-Wilson and Krizek, 2000; Krizek, 2003) (Figure 7; Supplemental Data Set 6). We performed the same analysis for ChIP-seq data available for BBM/PLT4 (Horstman et al., 2015), which resulted in a motif very similar to that for PLT2 (Figure 7A; Supplemental Data Set 6). In addition, PLT5 has been shown to be able to bind to an ANT-like motif (Yano et al., 2009). We identified the in vitro binding preference of PLT2 and PLT5, with ANT as a control, by SELEX (systematic evolution of ligands by exponential enrichment) (Tuerk and Gold, 1990; Haga et al., 2011) and confirmed that they all
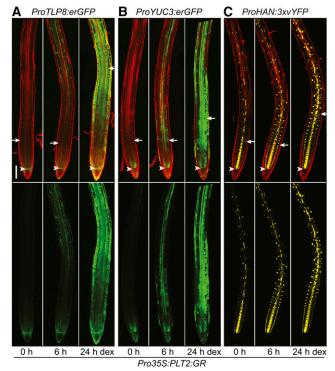

Figure 6. PLT2 Expression Pattern Influences the Boundary of Meristem Target Gene Expression Domains at the Root Tip.

Activation of ProTLP8:erGFP **(A)**, ProYUC3:erGFP **(B)**, and ProHAN:3xvYFP **(C)** expression in representative transgenic roots after 0, 6, and 24 h of DEX induction of PLT2-GR expressed under control of the constitutive 35S promoter in 5-d-old seedlings. For each induction series, a transgenic root is followed over time and depicted using identical confocal settings and the same medial focal plane. Experiments were repeated 26 times (ProTLP8:erGFP), 14 times (ProYUC3:erGFP), and eight times (ProHAN:3xvYFP). The lower panel depicts the green (GFP) channel only. Arrowhead indicates QC and arrow indicates shootward meristem boundary. Bar = 100 μm.
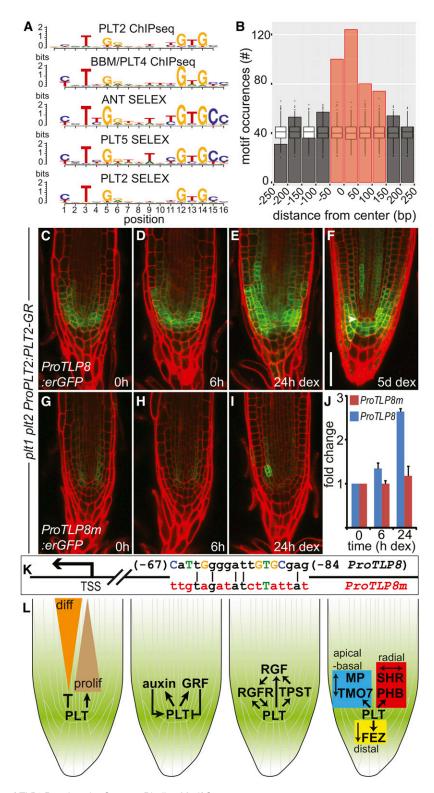
Figure 7. PLT2 Activation of *TLP8* Requires the Cognate Binding Motif Sequence.

(A) Alignment of the consensus motifs for PLT2 and BBM/PLT4 (ChIP-seq), and for ANT, PLT5, and PLT2 (SELEX). The *y* axis refers to the information content per motif position, measured in bits. See also Supplemental Data Set 6.

(B) PLT2 peaks assigned to regulated genes show enrichment for PLT2 motif occurrences compared with random genomic regions, and motifs were preferentially located close to the peak summit. PLT2 motif occurrences in PLT2 peaks were counted relative to peak summit positions. A region of 500 bp

recognize an ANT-like consensus motif (Figure 7A; Supplemental Data Set 6). Motif occurrences were enriched in PLT2 peaks assigned to regulated genes compared with random genomic regions and were preferentially located close to the peak summit (Figure 7B), consistent with a major role for this motif in mediating PLT2 binding and regulation.

Conservation and Functional Relevance of PLT Binding

Evidence for the functional relevance of PLT2 binding sites may be supported by the evolutionary conservation of bound regions serving regulatory functions across plant species (Haudry et al., 2013; Van de Velde et al., 2014; Heyndrickx et al., 2014). Accordingly, we found PLT2 binding sites to be present in conserved regions in dicotyledonous plants more than expected by chance, indicating that (part of) the PLT network is conserved (Supplemental Figures 7A to 7C). To confirm the critical role of PLT2 binding to a conserved DNA consensus sequence for target gene expression, we chose the promoter of *TLP8* (Figure 4C), which is short (~500 bp) and contains a single highly conserved PLT2 motif sequence (Supplemental Figures 5D and 5E). Mutagenesis of this sequence (Figure 7K) abolished both its expression and the response to PLT2-GR induction in a *plt1 plt2* background (Figures 7C to 7J), proving that motif DNA binding is necessary for PLT2 to drive appreciable *TLP8* expression levels.

DISCUSSION

The PLT transcription factors form a gradient that controls stem cell identity, meristem identity, cell expansion, and cell differentiation. Accordingly, we show in this study that around the stem cell niche, high PLT levels lead to a strong activation of growth and cell division genes (Figure 7L). Among the activated genes, 911 of 2028 genes show the highest expression in the L2 layer of the root, which is off the center of the highest PLT expression in the L1, and these genes are mainly expressed in the meristematic xylem (S4) tissue according to the root gene expression atlas. This set of genes also contributes the main overlap between the PLT and auxin response. However, 873 of these 911 genes are not recovered in the regulated target set, which is bound by PLT2. Although this may in part be due to sensitivity issues of the ChIP-seq, we do find a relatively high overlap of 30% activated bound genes compared with previous reports in the literature (LEAFY,

17% [Winter et al., 2011]; ABI3, 23% [Mönke et al., 2012]; KNOTTED1, 20 to 30% [Bolduc et al., 2012]; SPEECHLESS, 27% [Lau et al., 2014]), indicating that the regulated and not-bound gene set represents secondary PLT response genes. This result also suggests that part of the PLT response is directed via its effect on auxin biosynthesis, which results in the indirect activation of genes in the meristematic xylem of the L2 layer. This is in agreement with the sample time of the PLT regulated transcriptome at 6 h after induction, the rapid effect of PLT induction on auxin levels and biosynthesis genes within 2 h and the kinetics of this largest overlap of auxin response genes, which are induced by auxin within 2 to 4 h (Lewis et al., 2013). Nevertheless, previous experiments have shown that auxin application does not rescue the developmental defects observed in *plt1 plt2* mutant roots, indicating that auxin alone is not sufficient to bypass the requirement for *PLT* gene activity (Aida et al., 2004).

As PLT levels decrease along the root, the activation potential of the PLTs weakens and their repressive effect becomes less pronounced, allowing genes strongly enriched for cell expansion and cell type-specific differentiation to be upregulated in successively more shootward regions of the root. However, the higher overlap of bound and activated targets together with the highly enriched binding of PLT2 close to the transcription start site of activated genes versus only a slight enrichment observed for repressed genes compared with simulated random distributions indicates that PLTs mainly act as activators of transcription. Transcription activation tests in yeast are in agreement with these results. Therefore, repression may in part be indirectly controlled by PLT proteins, for example, involving PLT-activated repressive transcription factors. Nevertheless, we note that a part of the obtained binding peaks around repressed genes do contain PLT2 motifs. Both options can be tested through binding site mutation and its effect on gene regulation. The observed region-specific target gene activation by PLTs may be achieved by different threshold activation levels mediated by sequence context or position of binding sites (Chen et al., 2008; Levo et al., 2015), by cooperative interactions with tissue-specific transcription factors (Jolma et al., 2015), by indirect effects such as the local production and directed transport of auxin (this study), and by regulation of transcription factors implicated in growth and differentiation of specific tissues.

We identified the consensus binding motifs for PLT2 and BBM/PLT4 via de novo motif discovery in sequences under ChIP-seq

---

Figure 7. (continued).

centered at the peak summit and divided into 50-bp bins is depicted. Box plots display the distribution of motif occurrences considering random selections of 500-bp genomic regions. Red bars: enrichment over simulated random distribution, FDR < 5%.
(C) to **(E)** Induction of ProPLT2:PLT2-GR (0, 6, and 24 h DEX) in 5-d-old *plt1 plt2* mutant roots activates ProTLP8:erGFP expression. Experiments were repeated 12 times.
(F) Expression pattern of ProTLP8:erGFP in a *plt1 plt2 ProPLT2:PLT2-GR* seedling root germinated on DEX.
(G) to **(I)** Mutation of the PLT2 binding site in the *TLP8* promoter (*ProTLP8m*; see **[K]**) dramatically affects promoter activation by DEX induction of ProPLT2:PLT2-GR (0, 6, and 24 h DEX) in 5-d-old *plt1 plt2* mutant roots. Experiments were repeated six times.
(J) Expression of GFP quantified in roots of two representative independent ProTLP8:erGFP and ProTLP8m:erGFP transformants in a *plt1 plt2 ProPLT2: PLT2-GR* background. Expression is plotted in fold change of GFP levels relative to the uninduced (0 h) situation. Error bar indicates SD.
(K) Schematic representation of the *TLP8* promoter (*ProTLP8*) depicting consensus bases of the PLT2 binding motif in capitalized and colored letters. Red colored bases indicate mutated bases in *ProTLP8m*. Numbers indicate position relative to the TSS.
(L) PLT target genes regulate differentiation progression, regulatory feedback on PLT levels and patterning (Supplemental Table 1). Bar = 50 μm.

peaks and found very similar motifs by performing SELEX for PLT2, PLT5, and ANT. Furthermore, the consensus motif strongly resembles those observed for PLT1, PLT3, and, albeit somewhat less, for PLT7 obtained through DAP-seq (O'Malley et al., 2016). This suggests that all PLT/AIL members can bind to the same sequence motif, which is in agreement with the large overlap in regulated genes, their ability to (partially) complement *plt1 plt2* double mutants and the similar root phenotypes upon over-expression. In animal systems, the limited binding specificity of homeodomain transcription factors is known to be increased by their interaction with transcription factors of the TALE superfamily (Merabet and Mann, 2016). In a similar way, yet to be identified coregulators of PLT proteins may refine target specificity.

Our work identifies candidate PLT targets for several regulatory feedbacks (Figure 7L). Auxin induces *PLT* expression (Aida et al., 2004; Lewis et al., 2013; Mähönen et al., 2014), and here we show that PLT directly regulates polar auxin transport and auxin bio-synthesis genes, thereby elevating auxin levels. In addition, TYROSYLPROTEIN SULFOTRANSFERASE (TPST) and the Tyr-sulfated RGF peptides via their receptors (RGFR) induce and stabilize PLTs (Matsuzaki et al., 2010; Zhou et al., 2010; Ou et al., 2016; Shinohara et al., 2016), while *TPST*, *RGF*, and *RGFR* genes are regulated targets of PLT2 [Supplemental Table 1 and *ProRCH1(RGFR2)-erGFP* in Figure 5]. How are these feed-forward loops kept in check? A possible mechanism may be provided by GRF corepressors that were recently shown to control PLT levels in the root (Rodriguez et al., 2015). Here, we find that GRF2 is regulated by PLTs and bound by PLT2, suggesting a negative feedback loop for the stabilization of PLT levels. Finally, in line with the intriguing ability of PLT2 and BBM/PLT4 to initiate de novo organ formation in different developmental contexts, many genes involved in organ patterning are directly regulated by PLT2, such as *ARF5/MP*, *PHB*, *SHR*, and *FEZ*.

Each of the mechanisms by which PLT gradients are translated into graded gene expression responses can now be subjected to detailed investigation. Furthermore, the large set of genes regulated by PLTs presented here provide a rich data set to elucidate how cell state transitions for growth and differentiation are controlled at the cell and organ level. Finally, the evolutionary conservation of a considerable amount of relevant regulatory sequences in the PLT network will facilitate future studies on how meristematic control networks evolved within the Brassicaceae and, for a subset of well-conserved targets, in adjacent dicot families.

In summary, our data indicate how PLT gradients coordinate growth and differentiation through direct activation and (indirect) repression of target genes of which many have important roles in root development and of which several suggest distinct feedback controls on PLT activity. This information provides a molecular explanation for the local dosage-dependent effects of this plant transcription factor gradient in root development, which can now be detailed and tested in other developmental contexts.

METHODS

Plant Growth Conditions

Seeds were sterilized by liquid or vapor-phase methods, suspended in sterile 0.1% agarose, and cold-treated at 4°C in darkness for 2 to 5 d before plating (Clough and Bent, 1998; Heidstra et al., 2004). Unless otherwise stated, seeds were germinated on plates containing 0.5× germination medium (GM) agar: 0.5× Murashige and Skoog salt mixture, 1% sucrose, and 0.5 g/L MES, pH 5.8, in 0.8% agar. Plates were incubated in a near vertical position at 22°C and a cycle of 16 h light of ~110 μmol m^{-2} s^{-1}/8 h dark.

Plant Materials and Constructs

Genotype *plt1 plt2* refers to the *plt1-4 plt2-2* double mutant in the Wassilewskija (Ws) background (Aida et al., 2004). The *pGreen* binary vector set (Hellens et al., 2000) was used as a vehicle in *Agrobacterium tumefaciens*-mediated plant transformation [strain C58(pMP90); Koncz and Schell, 1986], with the floral dip method (Clough and Bent, 1998). Promoter and genomic sequences were amplified from Col-0 genomic DNA using the primer combinations listed below. *Pro35S:PLT2-GR*, *Pro35S:PLT5-GR*, *Pro35S:PLT3-GR*, and *Pro35S:PLT7-GR* were de-scribed previously (Galinha et al., 2007; Prasad et al., 2011; Hofhuis et al., 2013). *Pro35S:PLT1-GR* and *Pro35S:PLT4-GR* fusions were similarly generated by amplifying PLT genomic fragments, and these were cloned as *Sal*I-*Bam*HI into the plant binary vector *pGII227-GR* (hygromycin re-sistance in planta) for the generation of in-frame fusions with the rat GR fragment (Aoyama and Chua, 1997) under the control of the *35S* promoter and transformed into Col-0 wild-type plants.

For *PLT* complementing translational fusions to *GR*, *PLT5*, and *PLT7* genomic sequences were fused at the 3′ end to the C-terminal-encoding region of GR (Aoyama and Chua, 1997) and placed under the control of the 5.8-kb *PLT2* promoter using Gateway technology (Invitrogen) into a *pGreenII* vector conferring hygromycin resistance. Entry clones used are as described before (Galinha et al., 2007; Prasad et al., 2011; Mähönen et al., 2014). *plt1 plt2* harboring *PLT2* promoter-driven *PLT1-YFP*, *ProPLT2:PLT2-YFP*, *ProPLT2:PLT3-YFP*, or *ProPLT2:PLT4-YFP* was described previously (Galinha et al., 2007).

Promoter fragments of PLT2 target genes were fused to the *erGFP* coding sequence in a *pGreenII* vector, which was modified to harbor an attL4-attR1 cassette to allow cloning by way of Gateway recombination and which carried a methotrexate resistance cassette (Irdani et al., 1998) for selection in planta. The promoter of *TLP8* was fused to *erGFP* in a *pGreenII* based vector via Golden Gate cloning using the GreenGate modular system (Engler et al., 2008; Lampropoulos et al., 2013). The *TLP8* promoter with mutated binding site (*pTLP8m*) was constructed using overlapping primer PCR combined with GreenGate modules. Constructs were trans-formed into *plt1 plt2* plants carrying the *ProPLT2:PLT2-GR* inducible complementing vector.

For transcriptional autoactivation tests in yeast, the *PLT1* coding se-quence was amplified from cDNA and cloned into *pDONR221* by Gateway recombination and subsequently into *pDEST32* to create *pEXP32-cPLT1*.

Microscopy and Root Measurements

Light microscopy (Zeiss Axioscope) and confocal microscopy (Zeiss LSM 710) were essentially performed as described previously (Willemsen et al., 1998; Aida et al., 2004). Confocal images of median longitudinal sections were taken using a 10 μg/mL propidium iodide (Sigma-Aldrich) solution to visualize the cell walls. The root meristematic zone was determined by measuring from the QC to the first rapidly elongated cortex cell (Perilli and Sabatini, 2010), and the elongation zone by measuring from the first rapidly elongated cortex cell up to the point of the first emerging root hair. Meristem and elongation zone length as well as fluorescence levels were determined using ImageJ software.

Pro35S:PLTx-GR seedlings (Figures 1B and 1C; Supplemental Figures 1B and 1C) were germinated and grown on 0.5× GM agar plates and transferred at 5 d after germination to a plate with DMSO (mock) or 10 μM DEX (Sigma-Aldrich; 20 mM stock in DMSO). Roots were imaged after 6 h (mock and 6 h DEX time point) and 24 h of treatment. Sample size for each

data point for Figures 1B and 1C: Pro35S:PLT2-GR mock, 6 h DEX and 24 h DEX was *n* = 7, 19, and 13, respectively. Sample size for Supplemental Figures 1B and 1C data points: Pro35S:PLT1-GR *n* = 7 (mock) and *n* = 6 (24 h DEX), Pro35S:PLT3-GR *n* = 7 (mock) and *n* = 8 (24 h DEX), Pro35S:PLT4-GR *n* = 7 (mock) and *n* = 8 (24 h DEX), Pro35S:PLT5-GR *n* = 7 (mock), and *n* = 12 (24 h DEX), Pro35S:PLT7-GR *n* = 6 (mock), and *n* = 6 (24 h DEX). Light microscopy images were aligned and partially overlaid to generate a single root image using Adobe Photoshop. Care was taken to overlay two images at clearly visible characteristics in both. Contrast was adjusted for each image to that of the image it partially overlaid.

Complementation tests of the *plt1 plt2* double mutant short root phenotype were performed by growing genotypes *plt1 plt2 x ProPLT2:PLT1-YFP*, *ProPLT2:PLT2-YFP*, *ProPLT2:PLT3-YFP*, *ProPLT2:PLT4-YFP*, *ProPLT2:PLT5-GR*, *ProPLT2:PLT7-GR*, and wild-type Ws on 0.5× Murashige and Skoog agar plates (GM without sucrose) for 12 d. Lines harboring GR fusions were grown on plates with and without 10 μM DEX. Complemented seedlings from all genotypes together with Ws seedlings, and mock-treated *plt1 plt2 x ProPLT2:PLT5-GR* seedlings subsequently were aligned on a new agar plate for photography using a Nikon 3100 camera.

PLT2-induced expression of target promoters in the roots of 4- to 5-d-old seedlings was tested upon initial confocal analysis (0 h time point) followed by transfer to a plate with 10 μM DEX and reexamining expression in the same root after 6 and 24 h using identical confocal settings. Care was taken to image the same median focal plane while maintaining focus on particular characteristics observed in each root that was followed. Confocal images were placed on a black background and rotated to have the root pointing downward using Adobe Photoshop. For images in Figures 5 to 7 and Supplemental Figures 3A and 6, only the red channel was adjusted if needed to give the root the same appearance and intensity for each time point. The roots in Figures 2A and 6 and Supplemental Figure 6 were built up from partly overlapping confocal images that were merged and rotated to have the root point downward and placed on a black background using Adobe Photoshop. For the root in Figure 2A, global intensity was adjusted as a whole using Adobe Photoshop.

Promoter activity upon PLT2-GR induction (0, 6, and 24 h DEX) was quantified in two (ProTLP8:erGFP, ProTLPm:erGFP, and ProYUC3:erGFP) and three (ProRCH1:erGFP) representative independent transformants and depicted as fold change of erGFP levels relative to the uninduced situation. Experiments to determine promoter induction by DEX-induced *ProPLT2:PLT2-GR* in *plt1 plt2* roots were repeated four times (Pro*RCH1:erGFP*), 12 times (Pro*TLP8:erGFP*), six times (Pro*TLP8m:erGFP*), and nine times (Pro*YUC3:erGFP*). Experiments to determine ectopic promoter induction by DEX-induced *Pro35S:PLT2-GR* were repeated 26 times (Pro*TLP8:erGFP*), 14 times (Pro*YUC3:erGFP*), and eight times (Pro*HAN:3xvYFP*).

Whole Pro35S:PLTx-GR Seedling Transcriptomics

Pro35S:PLT[1,3,4,5,7]-GR seedlings were germinated on 0.5× GM agar and 4-d-old seedlings of each genotype were subsequently divided in batches (representing biological replicates) of ~50 seedlings into 50 mL liquid 0.5× GM in Erlenmeyer flasks. We chose the Pro35S:PLT4-GR line to be used as mock sample, and for this line additional Erlenmeyer flasks were prepared. Seedlings were cultured overnight under mild shaking (~75 rpm). The next day, DEX was added to each of the flasks to a final concentration of 10 μM, except the mock samples, to which an equal volume of DMSO was added. Each genotype was induced at 5-min intervals, which meant that all samples were harvested within half an hour to minimize the effect of time of day on the resulting transcriptome. After a 6-h induction, seedlings were quickly harvested through a sieve, transferred briefly onto paper towel, and flash frozen in liquid nitrogen. In summary, three biological replicates were generated for DEX-treated Pro35S:PLT[1,3,4,5,7]-GR seedlings, two biological replicates were generated for DEX-treated Pro35S:PLT3-GR seedlings, and four biological replicates were generated for mock-treated Pro35S:PLT4-GR seedlings.

In a separate experiment, Pro35S:PLT2-GR seedlings were treated as described above with DEX and, as a mock control, DMSO. For both DEX and mock treatment, three biological replicates were generated.

RNA was extracted from the seedlings using the Spectrum Plant Total RNA kit (Sigma-Aldrich) and used for microarray hybridization.

Fluorescence-Activated Cell Sorting of Root Protoplasts

To determine the PLT2-regulated transcriptome in the QC, we used the *plt1 plt2* line harboring the DEX-inducible complementing *ProPLT2:PLT2-GR* construct (Galinha et al., 2007) and introduced a *ProWOX5:erGFP* construct (Blilou et al., 2005) to allow QC cell sorting. Seeds were plated densely in three rows on square Petri dishes on 0.5× GM agar medium covered with nylon mesh (Sefar Nitex 03-15/10). At 5 d after germination, seedlings were transferred to new 0.5× GM agar plates containing 10 μM DEX in DMSO and incubated for 1 or 4 h. The control samples were transferred to new plates containing DMSO only and incubated for 1 h. After treatment, root tips were cut and harvested followed by protoplasting as described (Birnbaum et al., 2005). Root tips were placed inside cell strainers (70 μm) in Petri dishes containing protoplasting solution (50 mL of solution A [21.86 g mannitol, 150 mg KCl, 80 mg $MgCl_2$, 59 mg $CaCl_2$, 0.2 g BSA, and 78 mg MES in 200 mL water, set to pH 5.5, with 1 M Tris], 750 mg cellulase, and 50 mg macerozyme) and incubated for 1 h at room temperature with agitation. Protoplasts were collected by spinning down at 200*g*. The cells were subsequently washed and filtered through 70- and 40-μm cell strainers with 350 μL solution A. Protoplasts expressing GFP were isolated in a fluorescence-activated cell sorter (FACSAria II; BD Biosciences). The nozzle size was 100 μm. Cells were sorted in PBS (pH 7.4) as sheath fluid at an event rate of ~5000 to 10,000 events per second and a fluid pressure of 20 p.s.i. Upon excitation at 488 nm, GFP-expressing protoplasts were selected based on fluorescence emission in the green channel (530 nm with a band width of 30 nm) compared with negative controls. Cells were sorted into the RLT lysis buffer (Qiagen) supplemented with β-mercaptoethanol (1%), mixed, and flash frozen instantly. RNA was extracted from the sorted protoplasts with the RNeasy Micro Kit (Qiagen). Three independent biological replicates were performed for each time point.

Microarray Hybridization

Two microarray platforms were used for the transcriptomic analyses. Differential gene expression analysis for the QC cell-sorted physiological PLT2-GR induction experiment and for the whole-seedling Pro35S:PLT [1,3,4,5,7]-GR induction experiments was performed using the Affymetrix Arabidopsis ATH1 Genome Array. The whole-seedling Pro35:PLT2-GR induction experiment used the Arabidopsis Gene 1.1 ST Array plate. RNA quality was determined on a Bioanalyzer (Agilent). For the ATH1 microarray, RNA was amplified and labeled for analysis with the 3′ IVT Express Kit (Affymetrix), according to the manufacturer's instructions. In short, first-strand cDNA was synthesized using T7 oligo(dT) primer. The second cDNA strand was synthesized to generate a double-stranded cDNA template for transcription of the biotin-labeled cRNA. Labeled cRNA was fragmented before hybridization on an Affymetrix GeneChip Arabidopsis ATH1 Genome Array. For the AraGene 1.1ST microarray (Affymetrix), single-strand cDNA was prepared using the Ovation PicoSL WTA System V2 (NuGEN Technologies) according to the manufacturer's specifications. Labeling and fragmentation of the single-strand DNA was performed with the Encore Biotin Module (NuGEN Technologies). Hybridization and scanning of the biotinylated ss-cDNA samples onto the AraGene 1.1ST Array plate were performed with the GeneTitan (Affymetrix). Image analysis and extraction of raw expression data were performed with the Affymetrix Expression Console with "Gene-level Default: RMA-Sketch" settings. RNA processing and microarray hybridization were performed at ServiceXS (The Netherlands).

Yeast Autoactivation Assay

Yeast strain Y187 was transformed using the LiAc transformation protocol with *pEXP32-cPLT1* plasmid and, as an empty vector control, *pDEST32*, and selected for leucine autotrophy and growth. Positive colonies were subsequently restreaked on synthetic dropout medium lacking leucine and grown for 3 d at 28°C. The yeast was tested for autoactivation potential using a colony-lift assay according to the Yeast Protocols Handbook (Clontech). Images of the yeast plate and filter were cropped and rotated using Adobe Photoshop.

qRT-PCR

Pro35S:PLT2-GR seedlings were grown for 3 d on 0.5× GM agar plates with nylon membrane (Sefar Nitex 03-100/44). Seedlings were then transferred to 0.5× GM agar plates containing 10 μM DEX or a DMSO mock control. Root tips (3 to 4 mm) were collected after 4 h of treatment and transferred into liquid nitrogen immediately. Two biologically independent sets of samples were generated for each treatment. Total RNA was isolated from tissue samples using the Plant Total RNA kit (Sigma-Aldrich). Of each RNA sample, 1 μg was treated with DNase I (Fermentas) and reverse transcribed using the SuperScript III first-strand synthesis system (Invitrogen) according to the manufacturer's instructions. PCR amplification was performed in the presence of the double-stranded DNA-specific dye SYBR Green (Quantace). Amplification was monitored in real time with qRT-PCR performed using the 7900HT Fast real-time PCR system (Applied Biosystems) with three technical replicates. Expression levels were calculated relative to ACTIN2 (AT3G18780) using the $2^{-\Delta\Delta Ct}$ method. Statistical analysis was done in Microsoft Excel (ANOVA, single factor) using $P < 0.05$. Primers were designed according to the recommendations of Applied Biosystems.

Auxin Measurements

IAA quantification and biosynthesis measurements were performed as described (Ljung et al., 2005; Andersen et al., 2008). *Pro35S:PLT2-GR* seedlings were grown on vertical plates for 6 d in long-day conditions on 0.5× GM medium with 1% agar. The seedling roots were incubated in liquid 0.5× GM medium containing deuterated water (30% D2O) with and without 10 μM DEX for 2, 4, 8, 16, and 24 h. A control sample was also collected before incubation (0 h). The root tip (2 mm) was collected and root tips from 50 roots were pooled per sample. Then, 250 pg $^{13}C_6$-IAA was added to each sample as an internal standard before extraction and purification, and three replicates were analyzed for each time point and treatment. IAA was purified as described (Andersen et al., 2008) and analyzed using GC-MRM-MS. IAA synthesis rates were calculated as the ratio between labeled and unlabeled IAA, and IAA concentrations were calculated from the synthesis data as described (Ljung et al., 2005). A control experiment with wild-type Col-0 plants incubated for 8 and 24 h in the same medium showed no difference in IAA synthesis rates ± DEX treatment. For comparison of IAA levels between wild-type and *plt1 plt2 ProPLT2:PLT2-GR* seedlings, seedlings were grown on vertical plates as described above for 3 and 6 d after germination. No DEX was added to the plates resulting in the characteristic *plt1 plt2* mutant phenotype due to the absence of PLT2-GR activity. Root tips (100 × 2 mm) were harvested at 3 and 6 DAG for IAA quantification as described (Andersen et al., 2008). Then, 100 pg $^{13}C_6$-IAA was added to each sample as an internal standard, and five replicates were analyzed for each time point and genotype.

ChIP-Seq

Five milliliters of dry *Arabidopsis thaliana* seeds (*ProPTL2:PLT2-YFP*) was sterilized with chlorine gas for 8 h and stratified in 10 mL sterile MQ water for 48 h. Seeds were transferred to 0.5× GM agar plates topped with a nylon

mesh (Sefar Nitex 03-100/44) and grown for 4 to 5 d (~120 plates/ChIP). Root tips (~5 mm) were cut and transferred to PBS-S (PBS + 0.4 M sucrose). PBS-S medium was complemented with 1% (v/v) formaldehyde (16% methanol-free formaldehyde; Polysciences). A vacuum pump was used to reduce the pressure to ~0.2 atm three times within 5 min. Root tips were left to cross-link protein-DNA complexes for an additional 2 × 5 min. Cross-linking was stopped by the addition of 2 M glycine to a final concentration of 0.125 M followed by an incubation for 10 min at room temperature. Root material was washed three times in PBS-S and stored at −80°C. ChIP was performed as described by Song et al. (2014), with the following modifications: Ground samples were thawed in extraction buffer 1 (0.4 M sucrose, 10 mM Tris-HCl, pH 8.0, 5 mM β-mercaptoethanol, and protease inhibitor cocktail [cOmplete; Roche]) and passed through a double layer of Miracloth and pelleted. The nuclei-enriched pellet was treated twice with extraction buffer 2 (0.25 M sucrose, 10 mM Tris-HCl, pH 8.0, 10 mM MgCl$_2$, 1% [v/v] Triton X-100, 5 mM β-mercaptoethanol, and protease inhibitor cocktail [cOmplete]). After the second spin, the pellet was resuspended in 200 μL NLB (50 mM Tris-HCl, pH 8.0, 10 mM EDTA, 1% [w/v] SDS, and protease inhibitor cocktail [cOmplete]) and sonicated in a Bioruptor (Diagenode) for 2 × 5 min on low and 1 × 5 min on medium energy. In between sonication sessions, the water was cooled with ice. Then, 5 μL of anti-GFP antibody (AB290; Abcam) was used to coat 15 μL Protein-A Dynabeads (Invitrogen) in CDB (1.1% [v/v] Triton X-100, 1.2 mM EDTA, 16.7 mM Tris-HCl, pH 8.0, 167 mM NaCl, and protease inhibitor cocktail [cOmplete]) for 2 h at room temperature. Diluted ChIP samples and antibody-coated Dynabeads were incubated overnight at 4°C on a rotator. Beads were washed two times with low salt wash buffer (150 mM NaCl, 0.1% [w/v] SDS, 1% [v/v] Triton X-100, 2 mM EDTA, and 20 mM Tris-HCl, pH 8.0), one time with high salt wash buffer (500 mM NaCl, 0.1% [w/v] SDS, 1% [v/v] Triton X-100, 2 mM EDTA, and 20 mM Tris-HCl, pH 8.0), and two times with TE buffer (10 mM Tris-HCl, pH 8.0, and 1 mM EDTA). Beads were incubated with 100 μL TE + 1% SDS at 65°C on an Eppendorf Thermomix (800 rpm) for 15 min upon which the isolated DNA was purified using Zymo Research ChIP DNA cleanup (according to the manufacturer's instructions). Two biological replicate ChIP experiments were performed, and DNA from these experiments was pooled, and from this pooled DNA sample, two libraries were prepared and sequenced. In addition, the input sample was sequenced. Sequencing library preparation and subsequent SOLiD Sequencing were performed as described (Mokry et al., 2010).

SELEX

The *pGEX4T-1* plasmid (GE Healthcare) was used to construct and express GST-PLT5 fusion protein in *Escherichia coli* BL21. For GST-ANT and GST-PLT2 fusion proteins, appropriate sequences were cloned into *pDEST15* vector using Gateway technology (Invitrogen). For all transcription factors (TFs), full coding sequences were fused to the C-terminal part of GST. *E. coli* cells expressing GST-TF fusion protein were grown to the mid-log phase in Luria-Bertani broth containing ampicillin at 37°C and then for 24 h at 16°C in the presence of 1 mM isopropyl β-D-1-thiogalactopyranoside. Cells collected by centrifugation were suspended in PBS (pH 7.4) containing 0.5 mM PMSF. After the addition of Triton X-100 to a final concentration of 1%, cells were disrupted by a Bioruptor sonicator (Cosmo Bio). The lysate was mixed with one-tenth volume of 50% glutathione-Sepharose 4B beads (GE Healthcare) to bind GST-TF to the beads. Beads were washed extensively with a solution of PBS, 0.5 mM PMSF, and 0.1% Triton X-100. An oligonucleotide mixture containing 26 nucleotides of random sequence flanked by 24-nucleotide primer sequences on both sides (5′-GACATCACACTAGTCTAGAC- and ATGA-N26-TTCACCTTCA-GAACTGATGTACTC-3′) was converted into double-stranded DNA by PCR with PrimeSTAR HS DNA polymerase (Takara Bio) and used as R74

oligonucleotides. Glutathione-Sepharose 4B beads bound with GST-TFs were mixed with 100 ng of R74 oligonucleotides in binding buffer composed of 15 mM HEPES-KOH (pH 7.5), 6% glycerol, 2 mM DTT, 75 mM KCl, 0.5 mM EDTA, 50 ng/mL poly(dI-dC), 0.1% Triton X-100, and 0.5 mM PMSF at room temperature for 30 min with gentle shaking. Beads were washed with the binding buffer, and DNA was recovered from the beads by extraction with phenol:chloroform and ethanol precipitation. After amplification by PCR, 10 ng of DNA was subjected to the next round of selection by binding with GST-TF Sepharose 4B beads. After the selection step had been repeated 10 times, DNA fragments recovered from beads were cloned into the *Eco*RV site of pBlueScript I KS(+) (Stratagene) using *E. coli* DH5α. Colony PCR for more than 50 insertion-positive colonies was performed and their DNA sequences were determined.

Bioinformatics Data Analyses

Bioinformatic data analyses are described in detail in the supplemental data. The code used to generate the results from microarray and ChIP-seq experiments is available at the Figshare repository (https://dx.doi.org/10.6084/m9.figshare.3144553).

Accession Numbers

The microarray and ChIP-seq data from this study have been deposited in the National Center for Biotechnology Information's Gene Expression Omnibus repository (GEO: GSE79755). The accession numbers for *PLT* genes are as follows: *PLT1* (AT3G20840), *PLT2* (AT1G51190), *PLT3/AIL6* (AT5G10510), *PLT4/BBM* (AT5G17430), *PLT5/AIL5* (AT5G57390), and *PLT7/AIL7* (AT5G65510). The accession numbers for the other major genes mentioned in this study can be found in Supplemental Table 1.

Supplemental Data

Supplemental Figure 1. Shared properties of PLT proteins.

Supplemental Figure 2. Tissue expression profile of PLT-activated and -repressed genes.

Supplemental Figure 3. PLT2 regulates gene expression in the QC and auxin biosynthesis.

Supplemental Figure 4. PLTs regulate auxin response genes.

Supplemental Figure 5. PLT1 displays transcription activation activity.

Supplemental Figure 6. PLT2 overexpression shifts the boundary of the target gene expression domain.

Supplemental Figure 7. PLT2 binding sites are evolutionarily conserved.

Supplemental Table 1. Examples of PLT2-regulated targets with known function in Arabidopsis growth and development.

Supplemental Table 2. List of primers used for overexpression, GST fusion and promoter constructs and RT-PCR expression analysis.

Supplemental Material and Methods. Detailed description of bioinformatics data analysis.

Supplemental Data Set 1. Compendium of PLT-regulated differential gene expression.

Supplemental Data Set 2. GO term enrichment analysis on the PLT-regulated gene set.

Supplemental Data Set 3. Overlap between PLT-regulated genes and auxin-response genes.

Supplemental Data Set 4. PLT2 binding peaks from ChIP-seq and the overlap with BBM/PLT4 peaks.

Supplemental Data Set 5. PLT2 peaks and associated activated and repressed target genes.

Supplemental Data Set 6. Sequences of DNA fragments bound in ChIP and SELEX used to find the binding motif.

REFERENCES

Aida, M., Beis, D., Heidstra, R., Willemsen, V., Blilou, I., Galinha, C., Nussaume, L., Noh, Y.S., Amasino, R., and Scheres, B. (2004). The PLETHORA genes mediate patterning of the Arabidopsis root stem cell niche. Cell **119:** 109–120.

Andersen, S.U., Buechel, S., Zhao, Z., Ljung, K., Novák, O., Busch, W., Schuster, C., and Lohmann, J.U. (2008). Requirement of B2-type cyclin-dependent kinases for meristem integrity in *Arabidopsis thaliana*. Plant Cell **20:** 88–100.

Aoyama, T., and Chua, N.-H. (1997). A glucocorticoid-mediated transcriptional induction system in transgenic plants. Plant J. **11:** 605–612.

Bailey, T.L., and Elkan, C. (1995). Unsupervised learning of multiple motifs in biopolymers using expectation maximization. Mach. Learn. **21:** 51–80.

Bargmann, B.O., Vanneste, S., Krouk, G., Nawy, T., Efroni, I., Shani, E., Choe, G., Friml, J., Bergmann, D.C., Estelle, M., and Birnbaum, K.D. (2013). A map of cell type-specific auxin responses. Mol. Syst. Biol. **9:** 688.

Birnbaum, K., Jung, J.W., Wang, J.Y., Lambert, G.M., Hirst, J.A., Galbraith, D.W., and Benfey, P.N. (2005). Cell type-specific expression profiling in plants via cell sorting of protoplasts from fluorescent reporter lines. Nat. Methods **2:** 615–619.

Blilou, I., Xu, J., Wildwater, M., Willemsen, V., Paponov, I., Friml, J., Heidstra, R., Aida, M., Palme, K., and Scheres, B. (2005). The PIN auxin efflux facilitator network controls growth and patterning in Arabidopsis roots. Nature **433:** 39–44.

Bolduc, N., Yilmaz, A., Mejia-Guerra, M.K., Morohashi, K., O'Connor, D., Grotewold, E., and Hake, S. (2012). Unraveling the KNOTTED1 regulatory network in maize meristems. Genes Dev. **26:** 1685–1690.

Boutilier, K., Offringa, R., Sharma, V.K., Kieft, H., Ouellet, T., Zhang, L., Hattori, J., Liu, C.M., van Lammeren, A.A., Miki, B.L., Custers, J.B., and van Lookeren Campagne, M.M. (2002). Ectopic expression of BABY BOOM triggers a conversion from vegetative to embryonic growth. Plant Cell **14:** 1737–1749.

Brady, S.M., Orlando, D.A., Lee, J.Y., Wang, J.Y., Koch, J., Dinneny, J.R., Mace, D., Ohler, U., and Benfey, P.N. (2007). A high-resolution root spatiotemporal map reveals dominant expression patterns. Science **318:** 801–806.

Chen, C.C., Zhu, X.G., and Zhong, S. (2008). Selection of thermodynamic models for combinatorial control of multiple transcription factors in early differentiation of embryonic stem cells. BMC Genomics **9** (suppl. 1): S18.

Clough, S.J., and Bent, A.F. (1998). Floral dip: a simplified method for Agrobacterium-mediated transformation of *Arabidopsis thaliana*. Plant J. **16:** 735–743.

Engler, C., Kandzia, R., and Marillonnet, S. (2008). A one pot, one step, precision cloning method with high throughput capability. PLoS One **3:** e3647.

Galinha, C., Hofhuis, H., Luijten, M., Willemsen, V., Blilou, I., Heidstra, R., and Scheres, B. (2007). PLETHORA proteins as dose-dependent master regulators of Arabidopsis root development. Nature **449:** 1053–1057.

Haga, N., Kobayashi, K., Suzuki, T., Maeo, K., Kubo, M., Ohtani, M., Mitsuda, N., Demura, T., Nakamura, K., Jürgens, G., and Ito, M. (2011). Mutations in MYB3R1 and MYB3R4 cause pleiotropic developmental defects and preferential down-regulation of multiple G2/M-specific genes in Arabidopsis. Plant Physiol. **157:** 706–717.

Hardtke, C.S., and Berleth, T. (1998). The Arabidopsis gene MONOPTEROS encodes a transcription factor mediating embryo axis formation and vascular development. EMBO J. **17:** 1405–1411.

Haudry, A., et al. (2013). An atlas of over 90,000 conserved noncoding sequences provides insight into crucifer regulatory regions. Nat. Genet. **45:** 891–898.

Heidstra, R., and Sabatini, S. (2014). Plant and animal stem cells: similar yet different. Nat. Rev. Mol. Cell Biol. **15:** 301–312.

Heidstra, R., Welch, D., and Scheres, B. (2004). Mosaic analyses using marked activation and deletion clones dissect Arabidopsis SCARECROW action in asymmetric cell division. Genes Dev. **18:** 1964–1969.

Helariutta, Y., Fukaki, H., Wysocka-Diller, J., Nakajima, K., Jung, J., Sena, G., Hauser, M.T., and Benfey, P.N. (2000). The SHORTROOT gene controls radial patterning of the Arabidopsis root through radial signaling. Cell **101:** 555–567.

Hellens, R.P., Edwards, E.A., Leyland, N.R., Bean, S., and Mullineaux, P.M. (2000). pGreen: a versatile and flexible binary Ti vector for Agrobacterium-mediated plant transformation. Plant Mol. Biol. **42:** 819–832.

Heyndrickx, K.S., Van de Velde, J., Wang, C., Weigel, D., and Vandepoele, K. (2014). A functional and evolutionary perspective on transcription factor binding in *Arabidopsis thaliana*. Plant Cell **26:** 3894–3910.

Hofhuis, H., Laskowski, M., Du, Y., Prasad, K., Grigg, S., Pinon, V., and Scheres, B. (2013). Phyllotaxis and rhizotaxis in Arabidopsis are modified by three PLETHORA transcription factors. Curr. Biol. **23:** 956–962.

Horstman, A., Willemsen, V., Boutilier, K., and Heidstra, R. (2014). AINTEGUMENTA-LIKE proteins: hubs in a plethora of networks. Trends Plant Sci. **19:** 146–157.

Horstman, A., Fukuoka, H., Muino, J.M., Nitsch, L., Guo, C., Passarinho, P., Sanchez-Perez, G., Immink, R., Angenent, G., and Boutilier, K. (2015). AIL and HDG proteins act antagonistically to control cell proliferation. Development **142:** 454–464.

Irdani, T., Bogani, P., Mengoni, A., Mastromei, G., and Buiatti, M. (1998). Construction of a new vector conferring methotrexate resistance in *Nicotiana tabacum* plants. Plant Mol. Biol. **37:** 1079–1084.

Johnson, D.S., Mortazavi, A., Myers, R.M., and Wold, B. (2007). Genome-wide mapping of in vivo protein-DNA interactions. Science **316:** 1497–1502.

Jolma, A., Yin, Y., Nitta, K.R., Dave, K., Popov, A., Taipale, M., Enge, M., Kivioja, T., Morgunova, E., and Taipale, J. (2015). DNA-dependent formation of transcription factor pairs alters their binding specificity. Nature **527:** 384–388.

Koncz, C., and Schell, J. (1986). The promoter of TL-DNA gene 5 controls the tissue-specific expression of chimaeric genes carried by a novel type of Agrobacterium binary vector. Mol. Gen. Genet. **204:** 383–396.

Krizek, B.A. (2003). AINTEGUMENTA utilizes a mode of DNA recognition distinct from that used by proteins containing a single AP2 domain. Nucleic Acids Res. **31:** 1859–1868.

Krizek, B.A., and Eaddy, M. (2012). AINTEGUMENTA-LIKE6 regulates cellular differentiation in flowers. Plant Mol. Biol. **78:** 199–209.

Krizek, B.A., Bequette, C.J., Xu, K., Blakley, I.C., Fu, Z.Q., Stratmann, J.W., and Loraine, A.E. (2016). RNA-seq links the transcription factors AINTEGUMENTA and AINTEGUMENTA-LIKE6 to cell wall remodeling and plant defense pathways. Plant Physiol. **171:** 2069–2084.

Lai, C.P., Lee, C.L., Chen, P.H., Wu, S.H., Yang, C.C., and Shaw, J.F. (2004). Molecular analyses of the Arabidopsis TUBBY-like protein gene family. Plant Physiol. **134:** 1586–1597.

Lampropoulos, A., Sutikovic, Z., Wenzl, C., Maegele, I., Lohmann, J.U., and Forner, J. (2013). GreenGate—a novel, versatile, and efficient cloning system for plant transgenesis. PLoS One **8:** e83043.

Lau, O.S., Davies, K.A., Chang, J., Adrian, J., Rowe, M.H., Ballenger, C.E., and Bergmann, D.C. (2014). Direct roles of SPEECHLESS in the specification of stomatal self-renewing cells. Science **345:** 1605–1609.

Levo, M., Zalckvar, E., Sharon, E., Dantas Machado, A.C., Kalma, Y., Lotam-Pompan, M., Weinberger, A., Yakhini, Z., Rohs, R., and Segal, E. (2015). Unraveling determinants of transcription factor binding outside the core binding site. Genome Res. **25:** 1018–1029.

Lewis, D.R., Olex, A.L., Lundy, S.R., Turkett, W.H., Fetrow, J.S., and Muday, G.K. (2013). A kinetic analysis of the auxin

transcriptome reveals cell wall remodeling proteins that modulate lateral root development in Arabidopsis. Plant Cell **25:** 3329–3346.

Ljung, K., Hull, A.K., Celenza, J., Yamada, M., Estelle, M., Normanly, J., and Sandberg, G. (2005). Sites and regulation of auxin biosynthesis in Arabidopsis roots. Plant Cell **17:** 1090–1104.

Mähönen, A.P., ten Tusscher, K., Siligato, R., Smetana, O., Díaz-Triviño, S., Salojärvi, J., Wachsman, G., Prasad, K., Heidstra, R., and Scheres, B. (2014). PLETHORA gradient formation mechanism separates auxin responses. Nature **515:** 125–129.

Matsuzaki, Y., Ogawa-Ohnishi, M., Mori, A., and Matsubayashi, Y. (2010). Secreted peptide signals required for maintenance of root stem cell niche in Arabidopsis. Science **329:** 1065–1067.

Merabet, S., and Mann, R.S. (2016). To be specific or not: the critical relationship between Hox and TALE proteins. Trends Genet. **32:** 334–347.

Mokry, M., Hatzis, P., de Bruijn, E., Koster, J., Versteeg, R., Schuijers, J., van de Wetering, M., Guryev, V., Clevers, H., and Cuppen, E. (2010). Efficient double fragmentation ChIP-seq provides nucleotide resolution protein-DNA binding profiles. PLoS One **5:** e15092.

Mönke, G., Seifert, M., Keilwagen, J., Mohr, M., Grosse, I., Hähnel, U., Junker, A., Weisshaar, B., Conrad, U., Bäumlein, H., and Altschmied, L. (2012). Toward the identification and regulation of the *Arabidopsis thaliana* ABI3 regulon. Nucleic Acids Res. **40:** 8240–8254.

Nakajima, K., Sena, G., Nawy, T., and Benfey, P.N. (2001). Intercellular movement of the putative transcription factor SHR in root patterning. Nature **413:** 307–311.

Nawy, T., Bayer, M., Mravec, J., Friml, J., Birnbaum, K.D., and Lukowitz, W. (2010). The GATA factor HANABA TARANU is required to position the proembryo boundary in the early Arabidopsis embryo. Dev. Cell **19:** 103–113.

Nole-Wilson, S., and Krizek, B.A. (2000). DNA binding properties of the Arabidopsis floral development protein AINTEGUMENTA. Nucleic Acids Res. **28:** 4076–4082.

Nole-Wilson, S., Tranby, T.L., and Krizek, B.A. (2005). AINTEGUMENTA-like (AIL) genes are expressed in young tissues and may specify meristematic or division-competent states. Plant Mol. Biol. **57:** 613–628.

O'Malley, R.C., Huang, S.S., Song, L., Lewsey, M.G., Bartlett, A., Nery, J.R., Galli, M., Gallavotti, A., and Ecker, J.R. (2016). Cistrome and epicistrome features shape the regulatory DNA landscape. Cell **165:** 1280–1292.

Ou, Y., et al. (2016). RGF1 INSENSITIVE 1 to 5, a group of LRR receptor-like kinases, are essential for the perception of root meristem growth factor 1 in *Arabidopsis thaliana*. Cell Res. **26:** 686–698.

Perilli, S., and Sabatini, S. (2010). Analysis of root meristem size development. Methods Mol. Biol. **655:** 177–187.

Pinon, V., Prasad, K., Grigg, S.P., Sanchez-Perez, G.F., and Scheres, B. (2013). Local auxin biosynthesis regulation by PLETHORA transcription factors controls phyllotaxis in Arabidopsis. Proc. Natl. Acad. Sci. USA **110:** 1107–1112.

Prasad, K., et al. (2011). Arabidopsis PLETHORA transcription factors control phyllotaxis. Curr. Biol. **21:** 1123–1128.

Rodriguez, R.E., Ercoli, M.F., Debernardi, J.M., Breakfield, N.W., Mecchia, M.A., Sabatini, M., Cools, T., De Veylder, L., Benfey, P.N., and Palatnik, J.F. (2015). MicroRNA miR396 regulates the

switch between stem cells and transit-amplifying cells in Arabidopsis roots. Plant Cell **27:** 3354–3366.

Sabatini, S., Heidstra, R., Wildwater, M., and Scheres, B. (2003). SCARECROW is involved in positioning the stem cell niche in the Arabidopsis root meristem. Genes Dev. **17:** 354–358.

Sarkar, A.K., Luijten, M., Miyashima, S., Lenhard, M., Hashimoto, T., Nakajima, K., Scheres, B., Heidstra, R., and Laux, T. (2007). Conserved factors regulate signalling in Arabidopsis thaliana shoot and root stem cell organizers. Nature **446:** 811–814.

Schena, M., Lloyd, A.M., and Davis, R.W. (1991). A steroid-inducible gene expression system for plant cells. Proc. Natl. Acad. Sci. USA **88:** 10421–10425.

Shinohara, H., Mori, A., Yasue, N., Sumida, K., and Matsubayashi, Y. (2016). Identification of three LRR-RKs involved in perception of root meristem growth factor in Arabidopsis. Proc. Natl. Acad. Sci. USA **113:** 3897–3902.

Song, J., Rutjens, B., and Dean, C. (2014). Detecting histone modifications in plants. Methods Mol. Biol. **1112:** 165–175.

Tsuwamoto, R., Yokoi, S., and Takahata, Y. (2010). Arabidopsis EMBRYOMAKER encoding an AP2 domain transcription factor plays a key role in developmental change from vegetative to embryonic phase. Plant Mol. Biol. **73:** 481–492.

Tuerk, C., and Gold, L. (1990). Systematic evolution of ligands by exponential enrichment: RNA ligands to bacteriophage T4 DNA polymerase. Science **249:** 505–510.

Van de Velde, J., Heyndrickx, K.S., and Vandepoele, K. (2014). Inference of transcriptional networks in Arabidopsis through conserved noncoding sequence analysis. Plant Cell **26:** 2729–2745.

Wen, B., Nieuwland, J., and Murray, J.A. (2013). The Arabidopsis CDK inhibitor ICK3/KRP5 is rate limiting for primary root growth and promotes growth through cell elongation and endoreduplication. J. Exp. Bot. **64:** 1135–1144.

Willemsen, V., Wolkenfelt, H., de Vrieze, G., Weisbeek, P., and Scheres, B. (1998). The HOBBIT gene is required for formation of the root meristem in the Arabidopsis embryo. Development **125:** 521–531.

Winter, C.M., et al. (2011). LEAFY target genes reveal floral regulatory logic, cis motifs, and a link to biotic stimulus response. Dev. Cell **20:** 430–443.

Wysocka-Diller, J.W., Helariutta, Y., Fukaki, H., Malamy, J.E., and Benfey, P.N. (2000). Molecular analysis of SCARECROW function reveals a radial patterning mechanism common to root and shoot. Development **127:** 595–603.

Yano, R., Kanno, Y., Jikumaru, Y., Nakabayashi, K., Kamiya, Y., and Nambara, E. (2009). CHOTTO1, a putative double APETALA2 repeat transcription factor, is involved in abscisic acid-mediated repression of gibberellin biosynthesis during seed germination in Arabidopsis. Plant Physiol. **151:** 641–654.

Zhao, Y., Christensen, S.K., Fankhauser, C., Cashman, J.R., Cohen, J.D., Weigel, D., and Chory, J. (2001). A role for flavin monooxygenase-like enzymes in auxin biosynthesis. Science **291:** 306–309.

Zhou, W., Wei, L., Xu, J., Zhai, Q., Jiang, H., Chen, R., Chen, Q., Sun, J., Chu, J., Zhu, L., Liu, C.-M., and Li, C. (2010). Arabidopsis tyrosylprotein sulfotransferase acts in the auxin/PLETHORA pathway in regulating postembryonic maintenance of the root stem cell niche. Plant Cell **22:** 3692–3709.

Supplemental Data	**http://www.plantcell.org/content/suppl/2016/12/05/tpc.16.00656.DC1.html**
References	This article cites 65 articles, 32 of which can be accessed free at: http://www.plantcell.org/content/28/12/2937.full.html#ref-list-1
Permissions	https://www.copyright.com/ccc/openurl.do?sid=pd_hw1532298X&issn=1532298X&WT.mc_id=pd_hw1532298X
eTOCs	Sign up for eTOCs at: http://www.plantcell.org/cgi/alerts/ctmain
CiteTrack Alerts	Sign up for CiteTrack Alerts at: http://www.plantcell.org/cgi/alerts/ctmain
Subscription Information	Subscription Information for *The Plant Cell* and *Plant Physiology* is available at: http://www.aspb.org/publications/subscriptions.cfm